FT-Raman and infrared spectroscopic study of aragonite–strontianite ($Ca_xSr_{1-x}CO_3$) solid solution[1]

J.M. Alía [a,*], Y. Díaz de Mera [a], H.G.M. Edwards [b], P. González Martín [c], S. López Andrés [c]

[a] *E.U.I.T.A., Departamento de Química Física, Universidad de Castilla-La Mancha, Ronda de Calatrava 5, 13071 Ciudad Real, Spain*

[b] *Chemistry and Chemical Technology, University of Bradford, Richmond Road, Bradford, West Yorkshire BD7 1DP, UK*

[c] *Dpto. de Cristalografía y Mineralogía, Facultad de CC. Geológicas, Universidad Complutense, 28040 Madrid, Spain*

Abstract

Synthetic aragonite–strontianite solid-solution samples have been studied using dispersive IR and FT-Raman spectroscopy. In addition to the end-members, nine samples over a range of composition from $Ca_{0.9}Sr_{0.1}CO_3$ to $Ca_{0.1}Sr_{0.9}CO_3$ were analysed. Carbonate anion internal modes are examined in detail by means of band-shape analysis and component fitting procedures. Positional disorder induced by the random cationic substitution results in strong increase of the halfwidth in several vibrational bands. Results obtained for the doubly degenerate modes (antisymmetric stretching and bending, ν_3 and ν_4) reveal the presence of three components both in the IR antisymmetric stretching band as well as in the Raman antisymmetric bending band. These observations are interpreted in terms of an overtone $2\nu_4$ in possible Fermi resonance with the corresponding ν_3 fundamental in the IR spectra, and the presence of Davidov (factor group) splitting in the FT-Raman ν_4 band. Lattice modes in the FT-Raman spectra demonstrate weaker cohesion between the cation/carbonate/cation layers in aragonite (*synth*) than in strontianite (*synth*).

Keywords: FT-Raman; FTIR; Aragonite; Stronitianite; Fundamental modes

1. Introduction

In nature, the most important calcium carbonate polymorphs (calcite, rhombohedral, and aragonite, orthorhombic) are rarely encountered as chemically pure substances. Both crystal forms hold cationic changes that, in the case of aragonite substituted by strontium, can constitute an authentic solid solution. This solid solution has

* Corresponding author.

[1] Dedicated to the memory of Lucienne Couture, in the fiftieth anniversary of the publication of her extraordinary work 'Étude des spectres de vibrations de monocristaux ioniques', Annales de Physique, 12éme Série, t. 2 (Janvier–Février 1947) 5–94.

several interesting aspects. From the geochemical point of view, the introduction of small quantities (≈ 0.6 mol%) of strontium ion into the aragonite lattice increases the stability of the solid. In the same way, the stability of strontianite ($SrCO_3$) is strengthened by the presence of ca. 12.5 mol% of calcium ion [1]. Moreover, it seems energetically easier to introduce calcium ion into the strontianite lattice than vice versa. These results from synthetic samples are confirmed by the usual composition of the corresponding minerals: the strontium content in natural aragonite does not exceed 1–2 mol% [2], whereas strontianite can contain up to 25–30 mol% of calcium ion [3]. It is interesting to note that marine aragonite, with a strontium content of approximately 1 mol% [4], comes from sea-water with calcium/strontium molar ratios of $\approx 1200/1$ [5].

Casey et al. [6] studied the thermochemistry of the aragonite–strontianite solid solution and obtained an excess entropy of mixing which was very small or zero, supporting the existence of a regular solution. The value of such thermodynamic predictions goes beyond an academic interest; for example, in the Chernobyl nuclear accident some 37.50 km^2 were contaminated by radioactive material [7] comprising $^{90}Sr^{2+}$. Up to 70% of this metallic ion could have been fixed in the ground after reaction with the solid carbonates. On the other hand, the Sr:Ca ratio in coralline aragonite is often employed to determine the sea surface temperature in paleoclimate reconstructions [8]. Several authors have documented an inverse relationship between the temperature of the marine environment and the strontium uptake by coralline aragonite [5,9].

There have been numerous vibrational spectroscopic investigations of pure carbonates. After the comprehensive and often cited review of White [10], several collections of spectra of simple carbonates have been published. Herman et al. [11] have used a laser microprobe to obtain analytically the Raman spectra of natural carbonates. Griffith et al. [12] have recently published the first compilation of FT-Raman spectra of minerals, including several carbonates. However, papers dealing with double or mixed carbonates are more scarce [13]. From the seminal work of Adler and Kerr [14] who reported the IR spectra of a dozen of simple and double carbonates, Scheetz and White [15] published a detailed vibrational (Raman and IR) study of alkaline-earth double carbonates of natural origin that does not include species containing strontium ion. Moreover, only one of the minerals studied, alstonite [$CaBa(CO_3)_2$], is orthorhombic and could be considered structurally similar to the samples included in the present work. Gil et al. [16] studied several alkaline-earth simple carbonates with a high content Fe^{2+} by means of FT-IR spectroscopy. Böttcher et al. [17–19] have reported an interesting series of papers studying the changes promoted in the FT-IR spectra of the rhombohedral carbonates, $MgCO_3$ and $CaCO_3$, by the presence of other bivalent metallic ions such as Fe^{2+}, Mn^{2+} or Co^{2+}, which, in some cases (e.g. $FeCO_3$–$MgCO_3$) can form solid-solutions. These samples occur naturally and their vibrational study has been applied to geothermometry. The same group have published lately [20] and Raman and FT-IR spectra of synthetic α-$Na_2Ca(CO_3)_2$. To the best of our knowledge, there is no reference of similar studies for orthorhombic carbonates and, moreover, in only one case [12] has FT-Raman spectroscopy been employed.

In the present work, a series of synthetic samples of the solid-solution aragonite–strontianite, obtained by co-precipitation, is studied by means of IR (dispersive) and FT-Raman spectroscopy. Besides calcium carbonate and strontium carbonate, nine samples whose range of composition extends from $Ca_{0.9}Sr_{0.1}CO_3$ to $Ca_{0.1}Sr_{0.9}CO_3$ are analysed. The aim of this research is twofold: to assess spectroscopically the existence of the solid solution and to provide some data about the effect of the cationic positional disorder on the vibrational dynamics of the carbonate anion.

2. Experimental

2.1. Solids

Samples were prepared by the method of Plummer and Busenberg [1]. Briefly, for the synthesis of aragonites (lattice calcium ion mole fraction

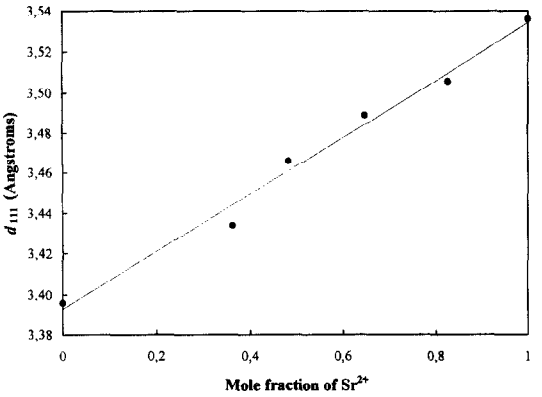

Fig. 1. Spacing for the [111] lattice plane in several samples of the synthetic aragonite–strontianite solid-solution.

between 0.5 and 1) different quantities of $SrCl_2$ were added to the base solution containing NaCl 0.43 M, $MgCl_2$ 0.078 M and $CaCl_2$ 0.10 M in order to obtain Sr^{2+} mole fractions of 0.1, 0.2, 0.3, 0.4 and 0.5, respectively. The solution was heated to 76 ± 0.5°C and the stoichiometric amount of carbonate as Na_2CO_3 (0.75 M) was added dropwise with vigorous stirring. On completion of the precipitation, the suspension was stirred for 1 h at the same temperature. The presence of NaCl and $MgCl_2$, as well as the moderately high temperature of reaction, are needed to avoid the precipitation of the calcite phase [21]. The preparation of strontianites (lattice strontium ion mole fraction between 0.5 and 1) was carried out in a similar way, but the initial $SrCl_2$ concentration was reduced to 0.05 M, with the corresponding amounts of $CaCl_2$ and Na_2CO_3. Precipitates were separated from the mother liquor through 0.65 μm Millipore filters, and washed repeatedly with deionized water until the elimination of Cl^- ion was confirmed (no reaction with $AgNO_3$). Afterwards, solids were dried by heating at 110°C for 48 h.

The chemical composition of the solids was determined by dissolution in 20% HCl at 60°C and atomic absorption spectrophotometric analysis. Maximum error over the theoretical stoichiometry was always less than 5%. The purity of the samples was confirmed by powder X-ray diffraction, scanning at 0.02 s^{-1} (2θ) using Cu–K_α radiation and silicon as an internal standard. A single-phase solid having the aragonite structure was always obtained in the synthesis. The spacing for the [111] lattice plane changes linearly with the strontium content, as can be observed in Fig. 1, in good agreement with the results reported by Casey et al. [6].

2.2. Vibrational spectra

FT-Raman spectra were excited at 1064 nm using an Nd:YAG laser and a Bruker IFS66 optical bench with an FRA 106 Raman accessory. Laser power was set at 70–80 mW and 1000 scans were accumulated with a resolution of 2 cm^{-1}.

Table 1
Factor group analysis of the carbonate ion in aragonite-type structures (*Pmcn*, D_{2h}^{16})

Free symmetry D_{3h}		Site symmetry C_s	Factor group D_{2h}	Activity
			A_{1g}	Raman
ν_1	A_1'	$A'[s(\sigma_x)]$	B_{3g}	Raman
			B_{1u}	Infrared
ν_2	A_2''		B_{2u}	Infrared
			B_{1g}	Raman
ν_3	E'	$A''[a(\sigma_x)]$	B_{2g}	Raman
			A_{1u}	Inactive
ν_4	E'		B_{3u}	Infrared

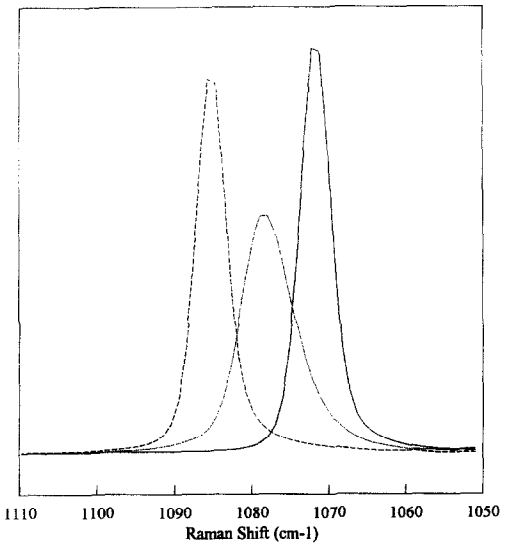

Fig. 2. Carbonate anion symmetric stretching band. Upper spectra: FT-Raman. Lower spectra: IR. From higher to lower wavenumber: aragonite (*synth*), equimolar sample and strontianite (*synth*).

Powdered samples were lightly pressed in the Bruker sample powder holder and mounted with 180° scattering geometry.

IR spectra were obtained using a Philips Pye Unican PU-9512 double-beam dispersive spectrophotometer. Each spectrum was recorded by co-addition of five scans between 2000 and 300

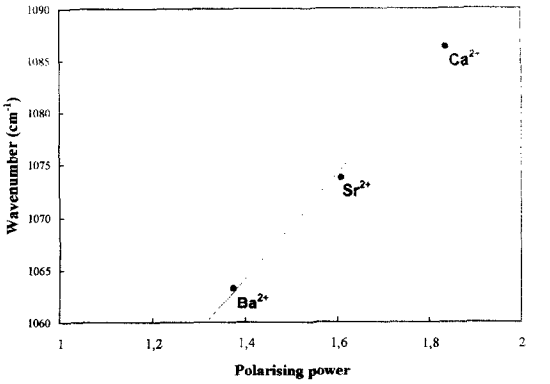

Fig. 3. Wavenumber of the carbonate anion symmetric stretching IR band plotted against the cation polarizing power, P [eV · (Å)$^{-1/2}$].

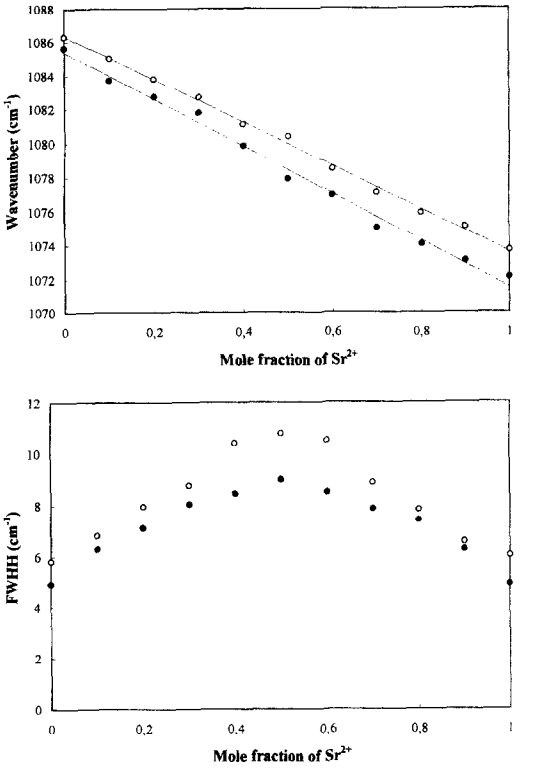

Fig. 4. (A) Wavenumber of the carbonate anion symmetric stretching band against the mole fraction of strontium ion in the solid. (○): IR spectra; (●): FT-Raman spectra. (B) Band halfwidth. Symbols as in (A).

Table 2
Line-fitting numerical results

Spectroscopy	Intercept	S.E.	Slope	S.E.	r	S.E.E.
FT-Raman	1085.4	0.24	−13.8	0.41	−0.9961	0.428
Infrared	1086.3	0.13	−12.7	0.23	−0.9986	0.238

Regression of the carbonate anion symmetric stretching band wavenumber against the mole fraction of Sr^{2+}. Intercept units, cm^{-1}; slope units, cm^{-1} Sr^{2+} mole fraction. S.E., standard error; S.E.E., standard error of estimate.

cm^{-1}. The scan speed was 90 cm^{-1} min^{-1}. Under these conditions, the precision was 1 cm^{-1}. Wavenumber accuracy was checked with the mixture indene/camphor/cyclohexanone [22]. Thirteen mm KBr disks (200 mg) containing ca. 0.5 mg of sample were used. Previously, the solids were moistened with *n*-propanol and ground very finely in an agate mortar, to minimise the Christiansen effect [23].

The mathematical (curve fitting) treatment of the spectra was carried out using the commercial software GRAMS/32® (Galactic Industries). Smoothing procedures or baseline correction routines were not applied in this work. All the figures in the paper are produced from integrated intensity-normalised spectra.

3. Results

3.1. Carbonate anion internal modes

The number and spectroscopic activity and symmetry of the carbonate anion normal modes in an aragonite-type crystal lattice (space group *Pmcn*) is shown in Table 1 [24,25].

3.1.1. Symmetric stretching, ν_1 (A'_1)

Fig. 2 shows the ν_1 fundamental in the FT-Raman and IR spectra of the end-members and the equimolar sample of the synthetic aragonite–strontianite[2] series. The wavenumbers obtained for aragonite (*synth*) and strontianite (*synth*) (IR: 1086.3 and 1073.7 cm^{-1}; FT-Raman: 1085.7 and 1072.0 cm^{-1}) agree with previous reports [10,12,26–28]. The asymmetry toward the lower wavenumbers is remarkable in the IR band of the end-members. However, such asymmetry is absent in the IR band of the equimolar sample and in all the FT-Raman bands. Davidov splitting could be invoked as a possible explanation of this asymmetry, because the theoretical analysis (see Table 1) predicts two IR active components with symmetries B_{1u} and B_{2u} arising from the free anion ν_1 (A'_1). The vibrational coupling between carbonate groups of adjacent layers is the origin of this marked asymmetry. The disorder induced by the presence of a second kind of cation, which is expected to be a maximum in the equimolar sample, would hinder this coupling and could explain the symmetry observed in the IR band of this sample.

It is possible to correlate the wavenumber of the FT-Raman ν_1 (A'_1) mode with the polarising power of the cation, as defined by Booker and Bredig [29]. Using the ionic radii listed by Shannon [30] for a coordination number of 8, which is probably more realistic for aragonite and aragonite-type structures than a coordination number of 6, the results can be observed in Fig. 3. Similarly, in the case of molten nitrates of monovalent cations reported by Booker and Bredig [29], the wavenumber diminishes when the polarising power decreases. However, the wavenumber corresponding to cerussite, ($PbCO_3$, 1053 cm^{-1}) [12] another orthorhombic carbonate, cannot be fitted by the same procedure because it is too low for the high polarising power of the lead ion [2.08 $eV \cdot (\text{Å})^{-1/2}$]. The reason for this discrepancy could lie in the partially covalent character of the carbonate/lead ion bond, to which Couture [25]

[2] In order to avoid confusion with the corresponding minerals and following the guidelines of the International Mineralogical Association [Bull. Mineral. 110 (1987) 717], the synthetic products studied in the present work are referred to as aragonite (*synth*) and stronitianite (*synth*). The absence of the abbreviation (synth) means that the reference is to the natural (mineral) substance.

has attributed the laminar structure of the mineral.

Fig. 4(a) shows the plot of the IR and FT-Raman ν_1 (A_1') band wavenumbers against the composition of the samples. In both cases the linear behaviour is evident, proving the existence of a solid phase unique with a monotonic compositional change, i.e. a regular solution, as predicted from the thermochemistry [6]. Table 2 gives the numerical results of the linear regressions obtained in this work; in both cases (IR and FT-Raman) and fittings are excellent and could be used with analytical purpose for similar samples.

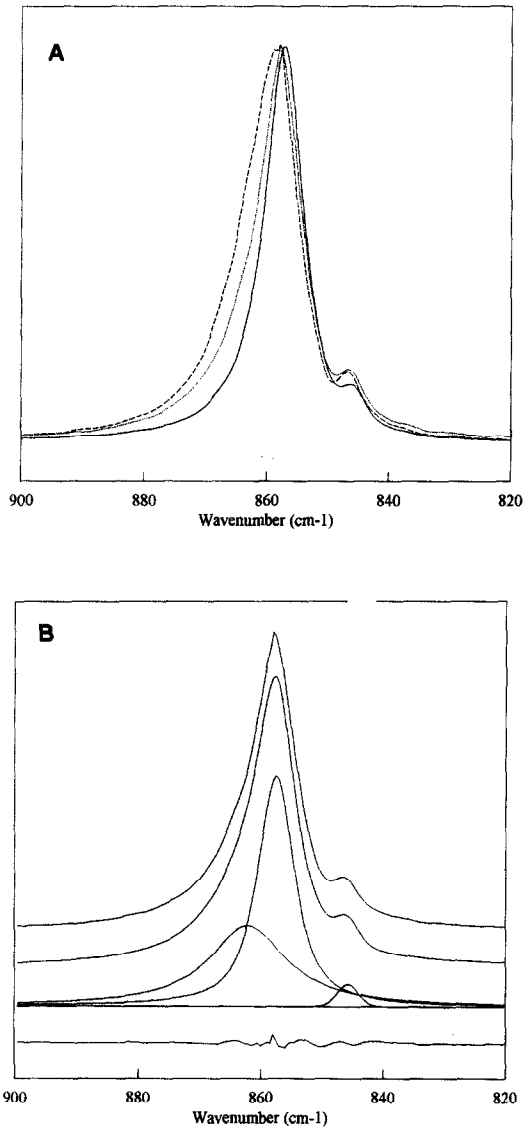

Fig. 5. (A) Carbonate anion out-of-plane bending IR band. Dashed line, aragonite (*synth*); dotted line, equimolar sample; full line, strontianite (*synth*). (B) Band deconvolution and component-fitting in the equimolar sample IR spectrum. From top to bottom: raw data, fitted spectrum, components and residual.

Table 3
Numerical results after the infrared band fitting of the carbonate anion out-of-plane bending band, ν_2:A_2''

Vibration[a]	Wavenumber (cm^{-1})	FWHH (cm^{-1})	Lorentz (%)
Satellite	846.7 (0.2)	6.5 (0.4)	92 (3)
B_{1u}	858.3 (0.4)	9.2 (0.5)	76 (7)
B_{2u}	865.4 (0.6)	14.2 (0.9)	81 (6)

Standard deviations are in brackets.
[a] Irreducible representations from Ref. [25].

Fig. 4(b) shows the evolution of the IR and FT-Raman ν_1 (A_1') band full-width at half-height (FWHH). The broadening reaches a maximum value in the equimolar sample, in which it is twice the value corresponding to the end-members. This remarkable increase in the bandwidth, due to the positional disorder induced by the random presence of a second cation, has previously been reported in the Raman spectra of double carbonates [15] and has been studied in detail by Bischoff et al. [31] in rhombohedral carbonates.

3.1.2. Out-of-plane bending, ν_2 (A_2'')

In the FT-Raman spectrum of aragonite (*synth*), this fundamental appears as a very small band (0.3% of the ν_1 (A_1') band integrated intensity) at 853 cm^{-1}, remaining undetected in the rest of the series. For this reason, the following results correspond only to IR spectra.

Fig. 5(a) shows this spectral region for the end-members and the equimolar samples. There is a very slight displacement of the maxima toward lower wavenumbers from the aragonitic value of 858 cm^{-1} to strontianite (*synth*) at 856.5 cm^{-1}. The very small influence of the cationic substitution on this normal mode, characteristic in orthorhombic carbonates, is in contrast with the corresponding rhombohedral carbonates where the out-of-plane bending is strongly dependent on

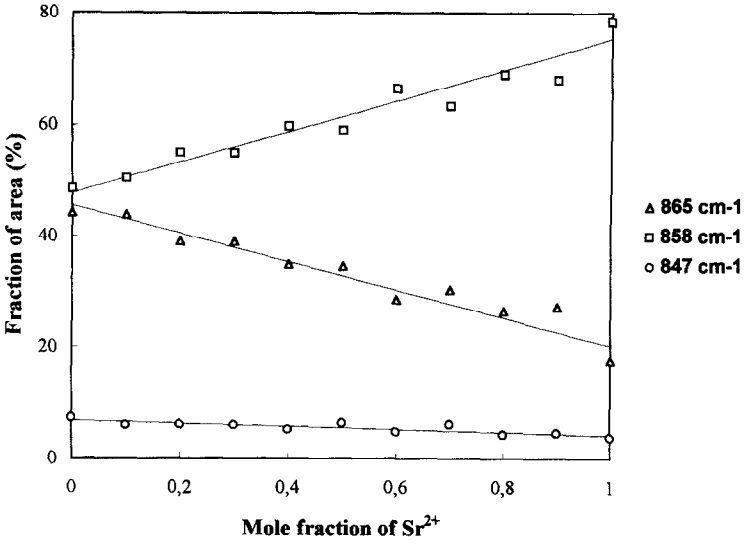

Fig. 6. Carbonate anion out-of-plane bending IR band. Fractions of area of the envelope components against the mole fraction of strontium ion in the solid.

the cation presence. In calcite-type structures, the cation is located on the same three-fold axis as the carbon atom of the carbonate ion. In such a way, during the out-of-plane bending vibration the carbon atom moves against the cation. The high degree of dispersion in the previously published data about this fundamental must be outlined. For aragonite, values of 870 and 875 cm^{-1} (apparent doublet) are reported by Huang and Kerr [26], whereas Donohue et al. [32] give a value of 853 cm^{-1}. Sterzel and Chorinsky [33] place this band at 857 cm^{-1}. For the strontianite, the wavenumber dispersion is also notable and, moreover, some authors [26] locate the band below the corresponding aragonite wavenumber (860 cm^{-1}), and others higher (857 cm^{-1} for Donohue et al. [32] and 859 cm^{-1} for Sterzel and Chorinsky [33]). Finally, Griffith [28] locates the band at 859 cm^{-1} in both species.

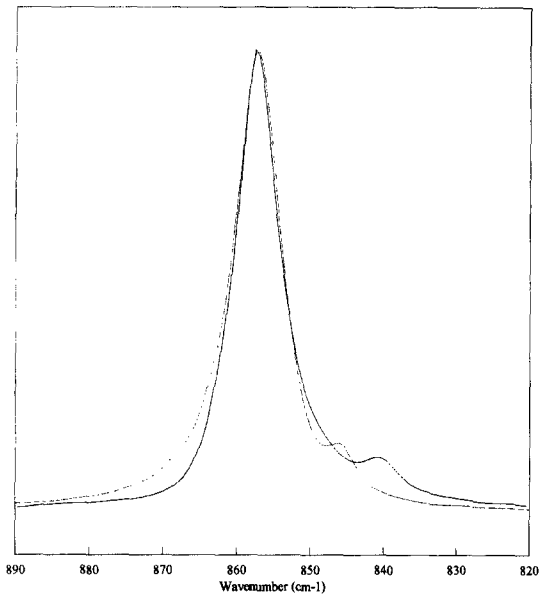

Fig. 7. Carbonate anion out-of-plane bending IR band. Dotted line, strontianite (*synth*); full line, witherite.

The weak band at ca. 847 cm^{-1}, sometimes called the satellite of the ν_2 band, is observable both in calcite-type carbonates as well as aragonite-type. Its assignment was quite controversial, generating abundant literature (see [10] for a detailed review), although at present its attribution to the $^{13}CO_3^{2-}$ isotopic anion, following the suggestion of Sterzel and Chorinsky [33], is generally accepted [20]. From IR reflectivity spectra, Frech and Wang [34] obtain the same symmetry species for the satellite and the main ν_2 band.

As can be seen in Fig. 5(a), the band is rather asymmetric toward the higher wavenumbers.

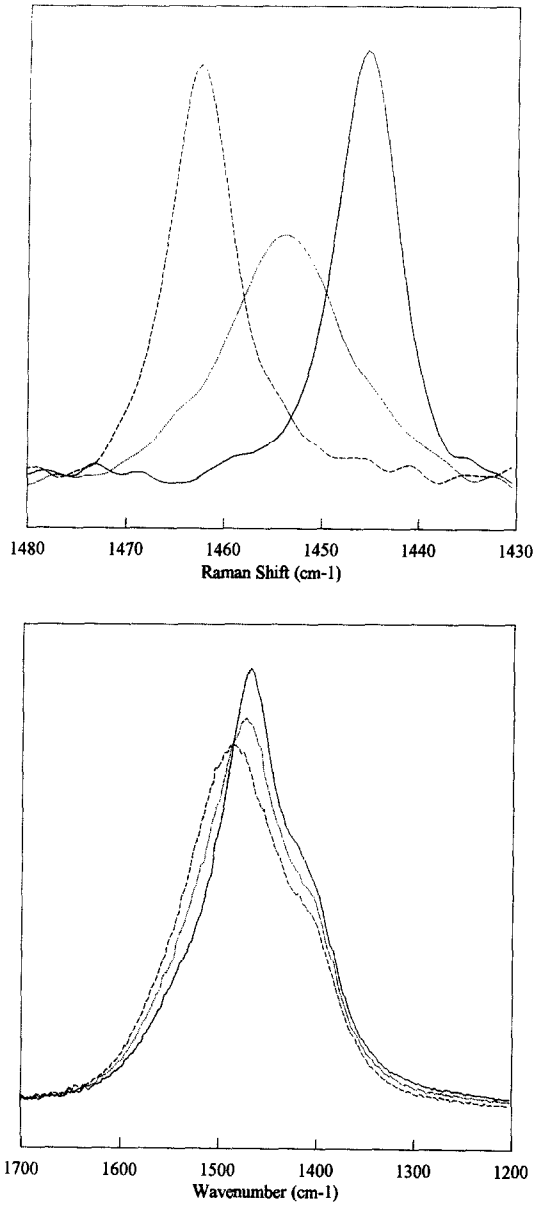

Fig. 8. Carbonate anion anitsymmetric stretching band. Upper spectra: FT-Raman. Lower spectra: IR. Dashed line, aragonite (*synth*); dotted line, equimolar sample; full line, strontianite (*synth*).

Band analysis and component fitting (Fig. 5(b)) reveals the presence of three components, whose characteristics are given in Table 3. The different assignments follow the proposal of Couture [25] for which the more intense band (~ 859 cm^{-1} in the present study and 866 cm^{-1} in the Couture's results) shows its moment in the *OZ* direction (type B_{1u}). As can be observed in Table 3, the different components retain their wavenumber and characteristics over the whole concentration range in the solid solution. The apparent narrowing and slight shifting toward the lower wavenumbers with increase in the strontium content (see Fig. 5(a)) are produced by the progressive predominance of the central component as the strontianitic end-member is reached. Fig. 6 shows the relative areas of the three components, to illustrate this effect. The intensity of the component assigned to B_{2u} symmetry is clearly lower in the strontianite (*synth*) than in the aragonite (*synth*) and must be explained. The appearance of a band in the IR spectrum means that the corresponding normal mode of vibration is allowed by the selection rules; IR absorption depends on the magnitude of the associated dipole moment change during the vibration and this can be affected by the cation presence. As has been already stated, the polarising power of the strontium ion is lower than that of corresponding calcium ion. The ap-

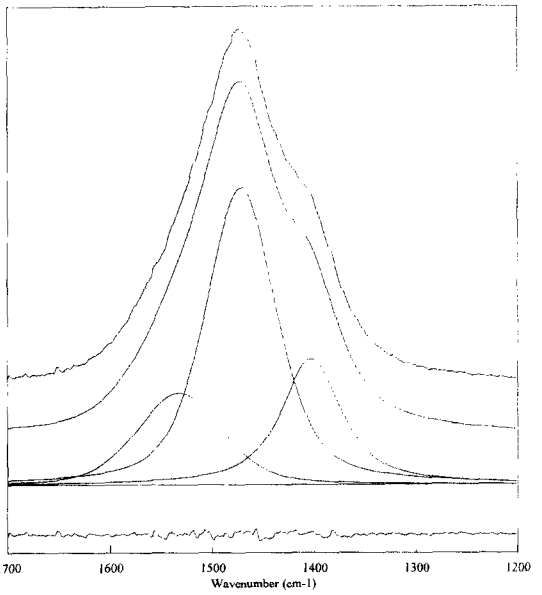

Fig. 9. Band deconvolution and component-fitting of the carbonate anion antisymmetric stretching IR envelope. Equimolar sample spectrum. From top to bottom: raw data, fitted spectrum, components and residual.

Table 4
Band-fitting results of the infrared $\nu_3(E')$ envelope

Sr^{2+} mol%	Component 1			Component 2			Component 3		
	ν	FWHH	%	ν	FWHH	%	ν	FWHH	%
0	1569.6	58.2	4.3	1489.5	107.5	78.8	1410.1	80.0	16.9
10	1565.6	66.8	6.8	1487.8	104.4	75.6	1409.0	83.8	17.6
20	1563.4	69.6	7.0	1486.0	99.0	64.1	1409.4	86.2	18.9
30	1559.4	76.8	10.1	1485.2	96.4	65.8	1408.3	86.0	24.1
40	1554.9	82.3	13.6	1481.4	90.3	65.5	1408.8	80.5	20.8
50	1551.9	78.3	13.0	1481.1	86.0	60.4	1407.6	83.2	26.5
60	1548.2	84.8	15.4	1478.2	80.8	59.2	1408.0	81.0	25.4
70	1544.4	90.0	16.7	1476.7	76.0	51.0	1407.6	84.7	32.3
80	1538.7	97.0	20.5	1473.7	72.4	45.2	1407.3	87.4	34.3
90	1534.7	99.1	20.9	1472.5	69.1	46.2	1407.0	83.1	32.9
100	1531.1	98.1	18.5	1469.2	64.3	48.6	1406.6	78.3	32.8

ν and FWHH, in cm^{-1}.

pearance of the B_{2u} mode, which is allowed by the selection rules, could be used to monitor changes in the dipole moment. Hence, the IR spectrum of witherite ($BaCO_3$) must show a $\nu_2(A_2'')$ band which is both symmetric and narrower than the corresponding band in strontianite (*synth*). Fig. 7 demonstrates this: witherite band is narrower (FWHH = 7.4 cm^{-1} against 8.7 cm^{-1} in strontianite (*synth*)) and is clearly symmetric.

3.1.3. *Antisymmetric stretching, $\nu_3(E')$*

In the FT-Raman spectra (Fig. 8), this fundamental appears as a single band of low intensity (ca. 1% of the symmetric stretching band). Its wavenumber changes linearly with the mole fraction of strontium ion from 1462 cm^{-1} in aragonite (*synth*) to 1446 cm^{-1} in strontianite (*synth*). These positions agree fairly well with previous reports [12,27,28]. The corresponding FWHH follow a similar trend to that described for the $\nu_1(A_1')$ band, namely 8.0 cm^{-1} in aragonite (*synth*), 13.5 cm^{-1} in the equimolar sample and 7.1 cm^{-1} in strontianite (*synth*).

The situation in the IR spectra is more complicated. From Fig. 8, it can be seen that when the strontium ion content is increased the general behaviour of the complex band can be summarised as follows: (1) shifting of the maximum toward lower wavenumbers ($\Delta\nu = -17$ cm^{-1}); (2) narrowing of the FWHH of the band from 145 to 112 cm^{-1}, more evident in the higher wavenumber region; (3) changes in the band asymmetry, which progressively becomes more pronounced at the lower wavenumbers. In order to quantify these changes, a band-fitting procedure has been carried out. Fig. 9 shows the result obtained from the analysis of the equimolar sample spectrum and Table 4 gives the numerical data corresponding to the complete series. The central component, whose wavenumber coincides with the reported value [10,27,28], is the most important along the series and is the responsible for the observed band profile narrowing. According to the theoretical analysis (see Table 1), up to three components can appear in the $\nu_3(E')$ region, with symmetries B_{1u}, B_{2u} and B_{3u}. It has been accepted [10,28] that the most intense band in the IR spectrum (at 1493 cm^{-1} in aragonite) would correspond to the B_{3u} symmetry. However, Frech and Wang [34] attribute a symmetry of B_{1u} to the stronger band and locates it at 1466 cm^{-1}. On the other hand, symmetry B_{2u} has been suggested [28] for the strontianite main band at 1470 cm^{-1} [26]. Recent calculations [35] predict the appearance of the three modes at 1506 (B_{1u}), 1504 (B_{2u}) and 1434 cm^{-1} (B_{3u}), respectively. We interpret our data as follows: the pair of components observed at higher wavenumbers (1570 and 1489.5 cm^{-1} in aragonite (*synth*); 1531 and 1469 cm^{-1} in strontianite (*synth*)) proceed from the doubly degener-

ate normal mode $\nu_3(E')$ which lifts its degeneracy under the effect of the crystalline field. The component at higher wavenumber in both systems could have ($B_{1u} + B_{2u}$) as its irreducible representation proceeding from the A′ component (see Table 1). The second member of the pair would have B_{3u} symmetry, proceeding from the A″ component. The corresponding splittings (80 cm^{-1} in aragonite (*synth*); 62 cm^{-1} in strontianite (*synth*)) are qualitatively comparable with those observed in the antisymmetric bending mode, $\nu_4(E')$, and will be discussed later. The third component, whose characteristics (position and FWHH) are independent of cationic substitution, is assigned the first overtone of one of the $\nu_4(E')$ components that practically does not change its wavenumber along the series (see later). Given its B_{3u} symmetry, the possibility of Fermi resonance with the antisymmetric stretching component must be taken into account; this could justify the intensity and breadth of the overtone. Moreover, in this way, two bands with symmetry B_{3u} would appear in this region, in complete agreement with the results published by Couture [25].

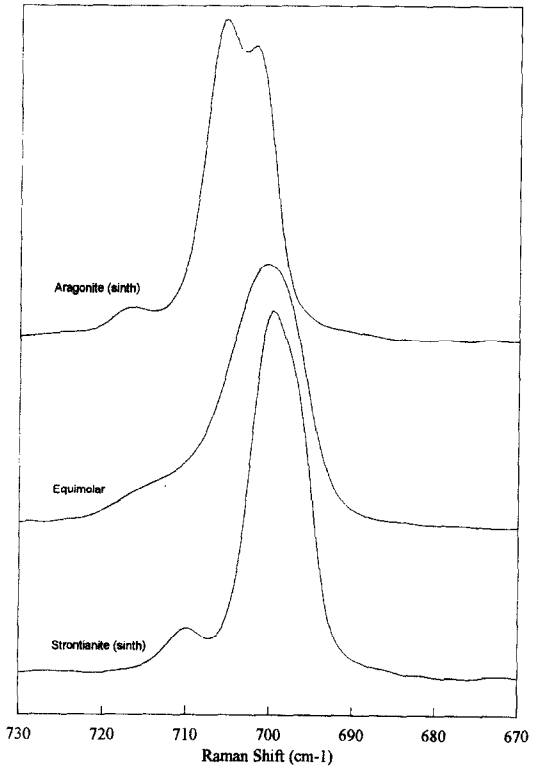

Fig. 10. Carbonate anion antisymmetric bending FT-Raman bands.

3.1.4. Antisymmetric bending, $\nu_4(E')$

Fig. 10 shows the FT-Raman spectra of several samples in the region of interest. Three maxima appear in the spectrum of aragonite (*synth*), while the strontianite (*synth*) spectrum reveals the presence of a shoulder in the lower wavenumber region of the stronger band. A weak feature at ca. 710 cm^{-1} is also evident which must not be confused with the ν_2 satellite as in this case, the band appears at a higher wavenumber than the main band and moves in wavenumber under the effect of the cationic substitution. There is considerable confusion in the literature with reference to this band. Several authors [12,26,28] report the presence of a single component in aragonite (703 or 705 cm^{-1}) as well in strontianite (700 or 702 cm^{-1}), although the presence of two components is also reported in aragonite: Couture locates the pair at 703 and 707 cm^{-1} and Behrens et al. [36] at 701 and 705 cm^{-1}. Up to four components (701, 705, 717 and 721 cm^{-1}) are observed in aragonite by Frech and Wang [34] who studied an oriented crystal. In the spectral assignment of Couture [25], the stronger components correspond to the irreducible representations B_{1g} (703 cm^{-1}) and A_{1g} (707 cm^{-1}) which originate from the originally doubly degenerate mode. The weak feature could correspond to the symmetries B_{2g} or B_{3g}, also allowed by the selection rules (see Table 1) and perhaps induced by pyramidal perturbation of the anion symmetry. The removal of degeneracy is less evident in the strontianite (*synth*), as it has been observed in the previous normal mode. The effect of the cation polarising power can be attributed again, because in witherite ($BaCO_3$) this mode appears as a single, symmetric band at 690 cm^{-1} accompanied by a minor feature at 700 cm^{-1} [15].

Results obtained after the component fitting are given in Table 5 and several points deserve comment. Although the shift toward the lower wavenumbers when the strontium ion content is increased is very similar for all the components, it

Table 5
Band-fitting results of the FT-Raman $\nu_4(E')$ envelope

Sr^{2+} mol%	Component 1			Component 2			Component 3		
	ν	FWHH	%	ν	FWHH	%	ν	FWHH	%
0	701.3	4.3	36.0	705.7	5.4	60.3	716.5	6.0	3.7
10	700.6	4.7	28.8	704.9	6.4	62.9	716.0	7.0	8.3
20	699.7	5.1	24.2	704.1	7.3	64.6	715.2	8.7	11.2
30	699.0	5.4	21.9	703.4	8.1	65.5	714.0	10.2	12.6
40	698.1	5.7	21.3	702.3	8.6	65.8	713.3	11.2	12.9
50	697.7	6.0	22.1	701.7	8.8	65.5	712.2	11.3	12.4
60	697.7	6.3	23.9	701.9	8.7	64.8	712.3	10.4	11.2
70	697.5	6.5	26.3	701.4	8.4	63.9	711.7	8.9	9.9
80	697.4	6.3	28.8	701.3	7.7	62.7	711.6	7.1	8.5
90	697.3	5.8	31.0	700.9	6.7	61.5	710.6	5.7	7.5
100	696.6	4.4	32.5	700.3	5.3	60.3	710.0	5.7	7.1

ν and FWHH, in cm^{-1}.

is slightly larger for the higher wavenumber component. These shifts, however, do not change linearly with the strontium ion content, as can be observed for the other normal modes. Starting from aragonite (*synth*), most of the wavenumber shift (66% in component 3 and 77% in component 1) has been achieved by the equimolar sample (Fig. 11). However, as in the case of the symmetric stretching mode, the broadening of the components also shows a maximum in the equimolar sample. These observations can be interpreted as the combined result of the increasing presence of strontium ion (a less polarising cation) in the aragonite lattice as well as the general disorder promoted by the cationic substitution.

Fig. 12 shows the IR spectra in the region of the antisymmetric bending mode. The lifting of the degeneracy is evident in the aragonite (*synth*) and strontianite (*synth*) spectra, although this does not result in a new weak feature equivalent to that observed in the FT-Raman spectra. This absence can be due to the coincidence in the wavenumber (712 cm^{-1}) to two (B_{1u} and B_{2u}) of the three components allowed in this region [37]. The third component (B_{3u}) would be located at 706 cm^{-1}. In the spectra discussed in this paper, the aragonite (*synth*) bands appear at 714 and 701 cm^{-1} and those corresponding to strontianite (*synth*) at 706 and 699 cm^{-1}. As in the case of the IR antisymmetric stretching band, the splitting is higher in the aragonitic term than in the strontianitic. The wavenumber of the first component decreases linearly when the strontium ion content increases, as can be observed in Fig. 11. However, the lower wavenumber component does not change its position significantly with the cationic substitution. For this reason, the first overtone of this component, whose symmetry is generally accepted as B_{3u} [25,35], remains at ca. 1400 cm^{-1} along the complete series. As we have suggested, this overtone could enter into Fermi resonance with the B_{3u} component of the complex IR antisymmetric stretching band. As in the FT-Raman spectra, the FWHH of both components suffers important changes: from 3.3 and 3.5 cm^{-1} in aragonite (*synth*) to 7.8 and 11.8 cm^{-1} in the equimolar sample, and decreasing to 5.4 and 4.9 cm^{-1} in strontianite (*synth*). Fig. 12 shows this band in the IR spectrum of witherite ($BaCO_3$) where, despite its aragonite-type structure (space group *Pmcn*), the degeneracy remains. Once again the influence of the polarising power of the cation on the spectral appearance of theoretically allowed components is evident.

3.2. Lattice modes

Fig. 13 shows the FT-Raman low frequency spectral region corresponding to the end-members of the solid solution. The enumeration and char-

acteristics of the resolved component are given in Table 6. In relation to aragonite, the coincidence with previous results [25,34] is good, taking into account that the present data were obtained from polycrystalline samples and the reference wavenumbers obtained from oriented crystal studies. To the best of our knowledge, there has not been any previous complete report of the external modes of strontianite. The coincidence with the scarce available data from polycrystalline samples [10,11] is noteworthy.

The external modes can be properly separated into two groups: translations of the ionic centres of gravity (considering the carbonate ion as a rigid entity) and anionic librations (restricted rotations). According to the theoretical analysis published by Couture [25], followed also by Frech and Wang [34], the stronger Raman bands must correspond to librations of the carbonate ion over

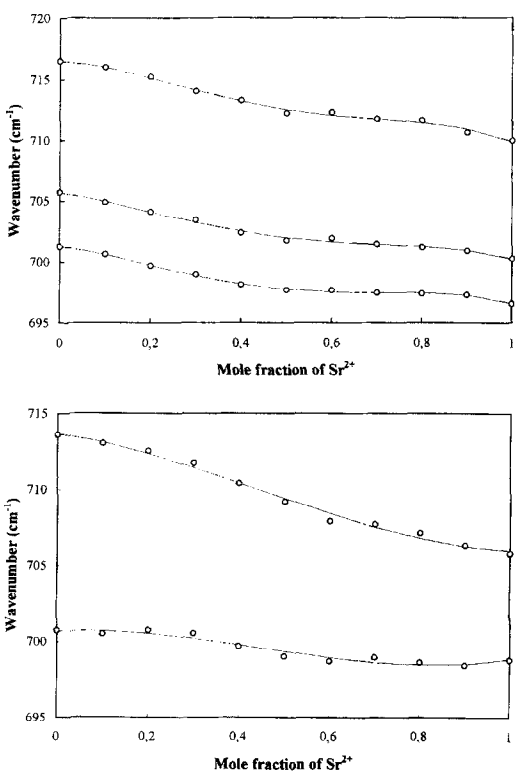

Fig. 11. Wavenumber of the carbonate anion antisymmetric bending band components. Upper: FT-Raman results. Lower: IR results.

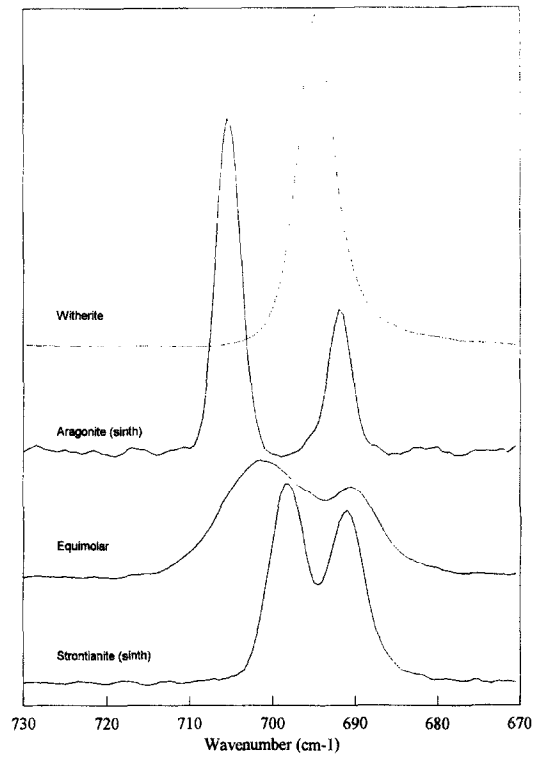

Fig. 12. Carbonate anion antisymmetric being IR bands.

the axes OY and OX which define the anion plane. The libration around the OY axis produces the most intense FT-Raman band in the region, whose wavenumber is at 153 cm^{-1} in aragonite (*synth*) and 148 cm^{-1} in strontianite (*synth*). The insignificant influence of the cation on the band wavenumber position is due to the fact that only three of the six first neighbour actions change in relative position with regard to the anion when it librates, because the restricted rotation is carried out along the C–O bond that coincides with the OY axis. This could explain also the higher wavenumber of the libration around the OX axis and the greater dependence of the cation present (aragonite (*synth*), 206 cm^{-1}; strontianite (*synth*), 181 cm^{-1}), because along this restricted rotation all the first neighbour cations change in relative positions.

There is a very good linear correlation when the wavenumbers corresponding to the ionic transla-

Table 6
Position and characteristics of the FT-Raman active external modes

Aragonite					Stontianite				
Wavenumber			FWHH	Intensity	Wavenumber			FWHH	Intensity
Couture [25]	Frech et al. [35]	Present work			White [11]	Herman et al. [12]	Present work		
		106.8	5.8	<1	105		102.0	7.0	5
113	112	115.4	14.5	8	119		114.8	8.2	7
	123	129.3	8.0	1	132		128.6	8.9	3
146	142	143.1	8.2	10	150	148	147.8	9.3	100
154.7	152	153.3	10.0	100			162.1	7.7	2.5
	161	163.5	4.8	1			170.8	7.0	5
183	180	180.6	8.0	10	183	183	180.6	12.0	70
193	190	191.3	11.2	10	220		214.6	3.8	<1
208.5	206	206.4	8.3	47			235.3	7.1	1.5
216.6	214	215.6	10.8	10	249	249	245.2	10.9	9
250	248	248.5	12.5	4			259.1	11.4	5
263		260.4	9.2	3					
276	272	272.3	12.5	5					
287	284	284.8	13.5	5					

tions in aragonite (*synth*) are plotted against the same values in strontianite (*synth*), as can be observed in Fig. 14. Among the components whose integrated intensities are greater than 1%, only two aragonite (*synth*) bands (216 and 248.5 cm^{-1}) seem to have no correlation in strontianite

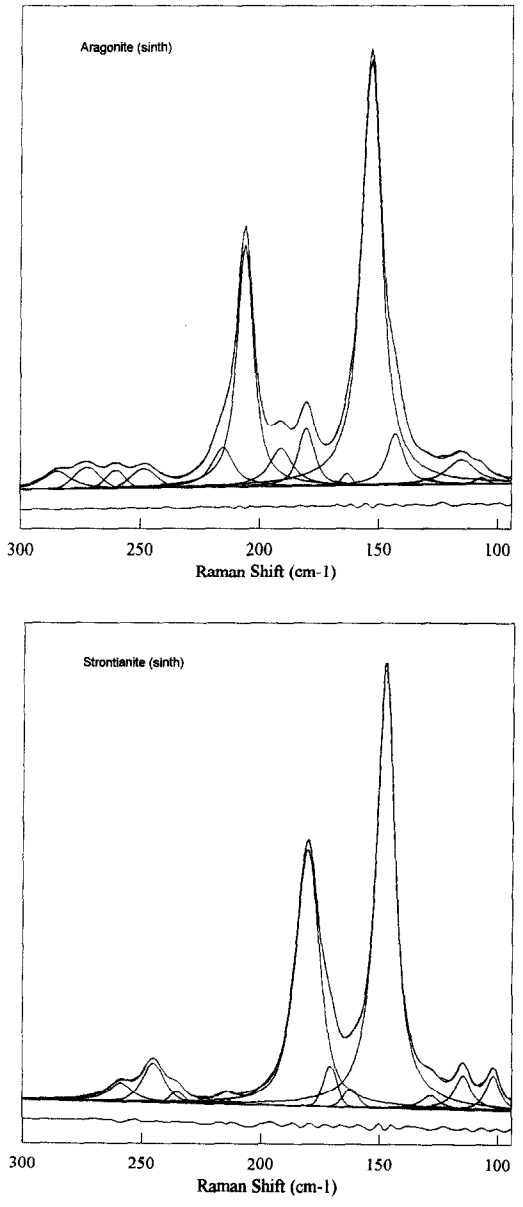

Fig. 13. Band deconvolution and component-fitting of the lattice modes FT-Raman spectral region. Residuals are shown below the spectra and fitted components.

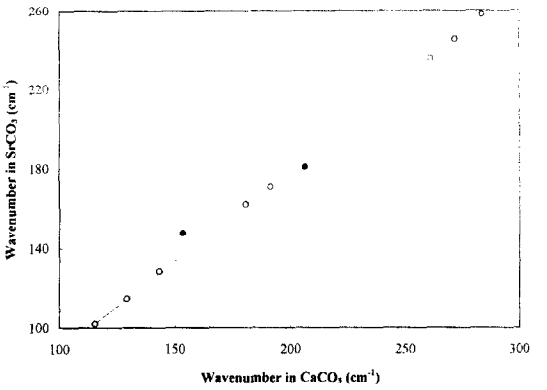

Fig. 14. Wavenumbers of the FT-Raman bands corresponding to the translations (○) and anionic librations (●) in synthetic samples of aragonite (abscissa) and strontianite (ordinate).

(*synth*). The bad fitting of the librational wavenumbers must be stressed. From the fitted data, the quotient

$$\frac{\nu_{\text{aragonite}}}{\nu_{\text{strontianite}}} = 1.115 \pm 0.010$$

can be calculated. As Couture [25] has demonstrated, the only forces that operate in this type of vibration (cohesion forces) are exerted between elementary layers (formed solely by cations or anions) and their neighbours and can be expressed as:

$$f = \nu^2 \cdot m$$

where f is the corresponding cohesion force, ν the frequency of the vibration and m the molecular mass. The ratio between the cohesion forces f_a and f_s in both aragonite (*synth*) and strontianite (*synth*) crystals can be calculated as:

$$\frac{f_a}{f_s} = \left(\frac{\nu_a}{\nu_s}\right)^2 \cdot \frac{m_a}{m_s} = (1.115 \pm 0.010)^2 \cdot \frac{100}{147.6}$$
$$= 0.843 \pm 0.016$$

which means that there is a stronger cohesion in strontianite (*synth*) than in aragonite (*synth*). This result is in confirmation with the higher thermodynamic stability of strontianite [38] and is close to the ratio calculated from macroscopic measurements (drop-solution enthalpies): 0.911 ± 0.011 [6].

The effect of the cationic substitution over the lattice modes can be observed in Fig. 15 which shows the FT-Raman 100–300 cm^{-1} spectral region in the samples with 10, 50 and 90% of strontium ion. As in the case of the internal modes a new feature is not observed, which suggests that the substitution is random. Apart from the shift of the maxima, a general broadening of the principal components is evident which, in the equimolar sample, results in a doubling of the halfwidths. Bishoff et al. [31], in their study of the Raman spectrum of synthetic calcite containing 15% of magnesium ion, reported the disappearance of all the lattice modes except for one band at 286 cm^{-1}. Something similar is observed by Böttcher and Reutel [20] in the Raman spectrum of synthetic α-$Na_2Ca(CO_3)_2$ (orthorhombic), where they report only a very broad and asymmetric band whose maximum is located at ca. 285 cm^{-1}. In the solid solution studied here, the cationic substitution seems to result in little perturbation of the lattice vibrationally, which is consistent with the X-ray diffraction results, experimentally and from a theoretical simulation [39].

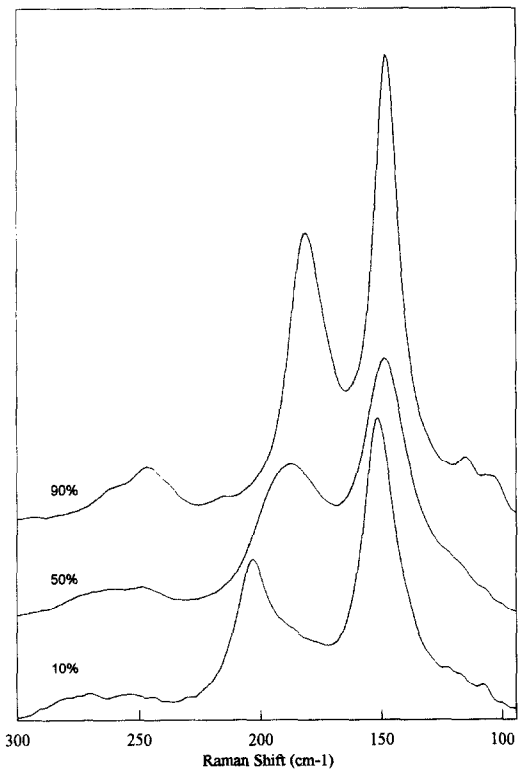

Fig. 15. External modes in the FT-Raman spectra of several samples of the synthetic solid solution aragonite–strontianite. Percentages correspond to the strontium ion content in the crystal.

4. Conclusions

The experimental results suggest the following four general conclusions.

(1) The vibrational (IR and FT-Raman) spectra of synthetic aragonite and strontianite are identical with those of their natural analogues, both in the carbonate anion internal modes as well as the external (lattice) modes.

(2) The progressive substitution of calcium ion by strontium ion has two main vibrational consequences: bandshifts toward the lower wavenumbers and significant broadening of the bands in the central terms of the series as a result of the positional disorder.

(3) The smaller polarizing power of strontium ion is revealed in the smaller distortion of several bands observable in the vibrational spectra of the strontianitic phases. Two arguments for this conclusion are the greater symmetry of the out-of-plane bending band in the IR, and the less-pronounced degeneracy lifting of the antisymmetric bending band in the FT-Raman for the strontianite (*synth*) spectra.

(4) The analysis of the lattice modes demonstrates that the interlayer cohesion is stronger in strontianite (*synth*) than in aragonite (*synth*) in good agreement with macroscopic (thermodynamic) observations. The low frequency region maintains its general characteristics over the composition range studied, which reflects the conservative character of the cationic substitution.

References

[1] L.N. Plummer, E. Busenberg, Geochim. Cosmochim. Acta 51 (1987) 1393.

[2] J.W. Morse, F.T. MacKenzie, Geochemistry of Sedimentary Carbonates, Elsevier, Amsterdam, 1990.
[3] J.A. Speer, Carbonates: minearalogy and chemistry, in: R. Reeder (Ed.), Reviews in Mineralogy, vol. 11, Mineralogical Society of America, 1983, pp. 145–189.
[4] D.J.J. Kinsman, H.D. Holland, Geochim. Cosmochim. Acta 33 (1969) 1.
[5] E.A. Jenne (Ed.), Chemical modeling in aqueous systems, ACS Symp. Series 93 (1979) 857–892.
[6] W.H. Casey, L. Chai, A. Navrotsky, P.A. Rock, Geochim. Cosmochim. Acta 60 (1996) 933.
[7] V.K. Lukashev, Appl. Geochem. 8 (1993) 419.
[8] S. de Villiers, G.T. Shen, B.K. Nelson, Geochim. Cosmochim. Acta 58 (1994) 197.
[9] S.V. Smith, R.W. Buddemeier, R.C. Redalje, J.E. Houcke, Science 204 (1979) 404.
[10] W.B. White, in: V.C. Farmer (Ed.), The Infrared Spectra of Minerals, The Mineralogical Society of America, 1974, pp. 227–284.
[11] R.G. Herman, C.E. Bogdan, A.J. Sommer, D.R. Simpson, Appl. Spectrosc. 41 (1987) 437.
[12] E.E. Coleyshaw, W.P. Griffith, R.J. Bowell, Spectrochim. Acta Part A 50A (1994) 1909.
[13] P.F. McMillan, A.M. Hofmeister, Spectroscopic methods in mineralogy and geology, in: F.C. Hawthorne (Ed.), Reviews in Mineralogy, vol. 18, Mineralogical Society of America, 1988, pp. 99–150.
[14] H.H. Adler, P.F. Kerr, Am. Mineral. 48 (1963) 839.
[15] B.E. Scheetz, W.B. White, Am. Mineral. 62 (1977) 36.
[16] P. Gil, A. Pesquera, F. Velasco, Eur. J. Mineral. 4 (1991) 521.
[17] M.E. Böttcher, P.-L. Gehlkenand, B. Usdowski, Contrib. Mineral. Petrol 109 (1992) 304.
[18] M.E. Böttcher, P.-L. Gehlkenand, B. Usdowski, Eur. J. Mineral. 4 (1992) 35.
[19] M.E. Böttcher, P.-L. Gehlken, N. Jb. Miner. Abh. 169 (1995) 81.
[20] M.E. Böttcher, C. Reutel, J. Raman Spectrosc. 27 (1996) 859.
[21] J.L. Bischoff, J. Geophys. Res. 73 (1968) 3315.
[22] Coblentz Society, Analyt. Chem. 47 (1975) 945A.
[23] J.D. Russell, in: V.C. Farmer (Ed.), The Infrared Spectra of Minerals, The Mineralogical Society, 1974, pp. 11–25.
[24] S. Bhagavantam, T. Venkatarayudu, Proc. Indian Acad. Sci. 9A (1939) 224.
[25] L. Couture, Ann. Phys. Ser. 12 (2) (1947) 5.
[26] C.K. Huang, P.F. Kerr, Am. Mineral. 45 (1960) 311.
[27] W.P. Griffith, Nature 224 (1969) 264.
[28] W.P. Griffith, J. Chem. Soc. A (1970) 286.
[29] M.H. Brooker, M.A. Bredig, J. Chem. Phys. 58 (1973) 5319.
[30] R.D. Shannon, Acta Crystallogr. A32 (1974) 751.
[31] W.D. Bischoff, S.K. Sharma, F.T. MacKenzie, Am. Mineral. 70 (1985) 581.
[32] M. Donohue, P.H. Hepburn, S.D. Ross, Spectrochim. Acta Part A 27A (1971) 1065.
[33] W. Sterzel, E. Chorinsky, Spectrochim. Acta Part A 24A (1968) 353.
[34] R. Frech, E.C. Wang, Spectrochim. Acta Part A 36A (1980) 915.
[35] A. Pavese, M. Catti, G.D. Price, R.A. Jackson, Phys. Chem. Mineral. 19 (1992) 80.
[36] G. Behrens, L.T. Kuhn, R. Ubic, A.H. Heuer, Spectrosc. Lett. 28 (1995) 983.
[37] R.E. Nyswander, Phys. Rev. 28 (1909) 291.
[38] L.N. Plummer, E. Busenberg, P.D. Glynn, A.E. Blum, Geochim. Cosmochim. Acta 56 (1992) 3054.
[39] P. González Martín, M. Sc. Thesis, Universidad Complutense, Madrid, 1997.